DESIGN, PROTOTYPING AND PRODUCTION OF THE VACUUM ASSEMBLY FOR EXPERIMENTS (VAX) FOR HL-LHC*

E. Barnes†, Y. Askar, V. Baglin, G. Bregliozzi, P. Chiggiato, P. Costa Pinto, Y. Delaup,
J. Perez Espinos, A. T. Perez-Fontenla, CERN, Geneva, Switzerland

Abstract

For the High-Luminosity LHC (HL-LHC), the Vacuum Assembly for eXperiments (VAX) of the ATLAS and CMS experiments required a major redesign to improve accessibility and reduce personnel exposure to radiation during its exploitation and maintenance. In the current LHC configuration, the VAX is located at a closed end of the tunnel, where the risk of oxygen-deficiency is also present. To address these safety concerns, the VAX modules have been relocated to the opposite side of the TAXS absorber, within the experimental cavern. This new layout enables fully remote installation, connection and removal of the VAX modules using a robot suspended from a crane, in line with ALARA (As Low As Reasonably Achievable) radiation exposure principles. It also allows the first quadrupole magnet to be positioned 833 mm closer to the interaction point, improving the final focusing of the beams before collisions.

This paper presents the design, prototyping, and production of the VAX, with a focus on the development of a key vacuum component: the DN80 universal joint bellows. Given the novel application of thin-film coatings to these elements, in particular the use of amorphous carbon (a-C), an emphasis is placed on the coating qualification.

INTRODUCTION

An overview of the HL-LHC beam vacuum layout of the CMS experiment is shown in Fig. 1. The VAX modules M1 and M3 allow isolation of the LHC beam vacuum system and the experimental beam vacuum system by means of DN80 sector valves, with M1 containing a cold cathode gauge which measures the pressure at the extremity of the inner triplets. In addition, the decoupling of the unbaked and baked vacuum sectors is made possible by the M1 sector valve. This distinction is important for coating selection: amorphous carbon (a-C) coatings can be used in unbaked sectors, whereas non-evaporable getter (NEG) coatings require baking for activation [1].

M2 has a DN40 angle valve to allow neon venting, pump-down and vacuum commissioning during NEG activation of the ATLAS and CMS experiments. A rupture disk is also installed in M2 to protect the experimental vacuum chambers in case of a helium inrush from the inner triplets. Additionally, M2 is the only module allowing flexibility, with M1 and M3 fixed to the TAXS and experimental chambers respectively [2]. As a result, the bellows of M2, connecting to M1 and M3 must accommodate any misalignments as well as the relative movement between the LHC tunnel and the experimental caverns, measured at 0.2 mm/year in ATLAS [3], [4].

Finally, the Q1-TAXS module accommodates for any misalignment between Q1 and the TAXS chamber, as well as subsequent adjustment using Full Remote Alignment System (FRAS), introduced for the first time as part of the HL-LHC upgrade [5]. This area is expected to be maintenance-free; as a result, external bellows defining a secondary volume, equipped with a pumping port, are foreseen to mitigate the impact of a potential leak on the inner bellow [6].

MECHANICAL DESIGN OF THE UNIVERSAL JOINT BELLOWS

Due to limited accessibility for maintenance, any forced intervention in this region would have a significant impact

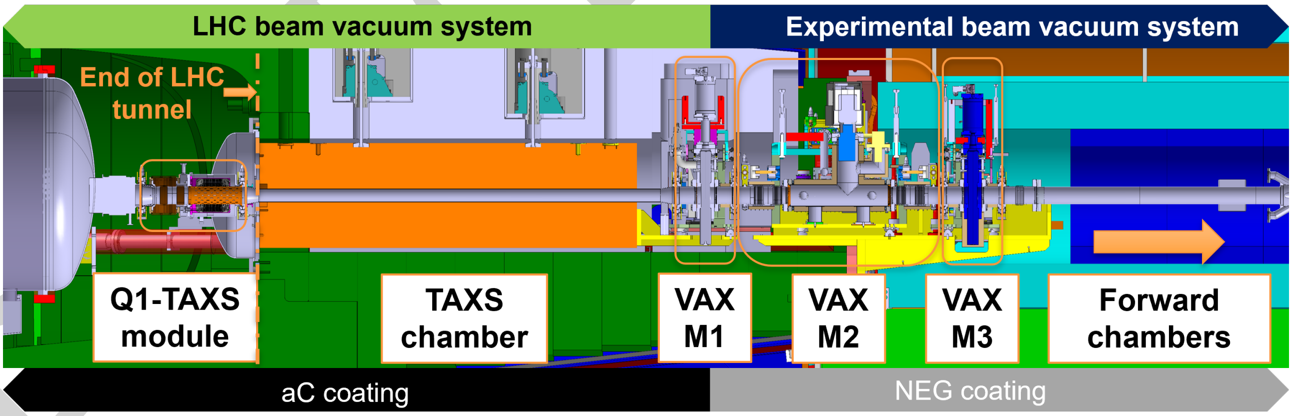

Figure 1: HL-LHC beam vacuum layout at experiment to collider interface area (Example from the left side of CMS).

---

* Work supported by the HL-LHC project

† edward.barnes@cern.ch

on machine operation, making it particularly critical for system reliability. Consequently, the bellows were designed without RF fingers, leaving the convolutions directly exposed to the beam. The geometry of the convolutions can induce beam instabilities and power loss. To address this, the convolution height, pitch, and number were optimised with respect to both beam impedance and mechanical performance [7], [8].

The universal joint bellows were mechanically designed to meet the following specifications, which enables use in both the Q1-TAXS and M2, ensuring reliable operation for at least 500 cycles at temperatures up to 250 °C:

- ±5 mm transverse offset
- −25 mm axial compression (not under vacuum)
- +15 mm axial extension.

THIN-FILM COATING OF BELLOWS

Applying thin-film coatings to the bellows in this region of the accelerator is necessary to reduce the secondary electron yield (SEY) of their surfaces, thereby mitigating the risk of electron cloud formation and electron multipacting. The VAX is located approximately 17–21.5 m from the IP, a region particularly susceptible to these effects. Here, counter-rotating beams circulate within a common vacuum chamber, effectively halving the bunch spacing and increasing the likelihood of electron cloud formation. In addition, electron-stimulated desorption can lead to beam loss, equipment irradiation, and elevated background levels within the experiments [9].

Two coatings were implemented: a-C for the Q1-TAXS, and NEG for M2. In the LHC, the copper RF inserts are typically coated rather than the bellows themselves. Consequently, this work represents the first application at CERN of a-C coating directly to bellows, as well as the first instance of NEG coating being applied to stainless-steel bellows in the LHC.

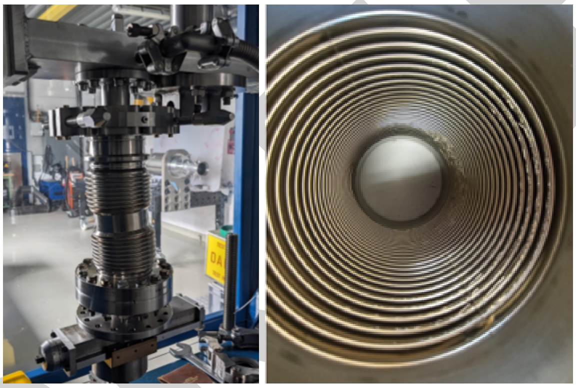

Figure 2: Fatigue testing bellows until failure (left). NEG peel-off on early prototype (right).

One of the principal challenges in coating these components was achieving reliable adhesion of the thin-film coatings throughout the operational lifetime of the bellows. By design, bellows must accommodate large deformations and high strain, which impose significant mechanical stresses on the coating. To qualify the coating process for production, prototype bellows were subjected to a series of tests, as described below:

- Five cycles of NEG activation, saturation, and venting.
- Mechanical testing to the required specification (see Fig. 2).
- A further three cycles of NEG activation, saturation, and venting.
- Mechanical cycling until failure.

The mechanical cycling to failure exceeded the specified requirements by more than a factor of five in terms of the number of cycles. In addition, the applied deformation exceeded the maximum expected operational levels by up to 50%. The bellows were repeatedly extended and compressed by up to ±35 mm under vacuum conditions, combined with a transverse offset of up to ±8 mm. The a-C-coated bellows were also subjected to thermal cycling up to 250 °C, to introduce additional stress to the coating.

Early prototypes exhibited NEG peel-off during mechanical cycling, which can be observed on the right side of Fig. 2. To mitigate this issue, inverse ion sputtering was introduced to remove a few nanometres of stainless steel from the surface, thereby breaking down any surface oxide prior to the application of the thin film coating by DC magnetron sputtering. This treatment effectively resolved the adhesion issue, as the thin films remained adherent throughout mechanical and thermal cycling until failure of the bellows. Following failure of the prototype bellows, the thickness distribution of the coatings across the convolutions of the bellow was analysed.

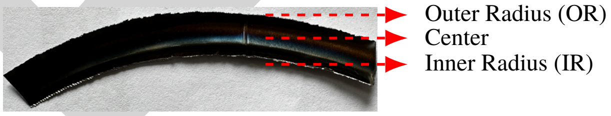

Figure 3: Position of FIB cuts on the a-C coated sample [10].

Samples were characterised at three locations on a convolution seen in Fig. 3:

- Outer Radius (OR): the position on the convolution furthest from the sputtering source.
- Centre: an intermediate location between the OR and IR.
- Inner Radius (IR): the position on the convolution closest to the sputtering source.

Coating thickness was measured on convolution cross-sections prepared using focused ion beam (FIB) milling and analysed by scanning electron microscopy (SEM). The platinum layer visible in Fig. 4 was deposited solely to protect the coating during FIB milling.

For reference, if applied to a smooth cylindrical surface, the expected coating thickness would be approximately 1 µm for NEG and 400 nm for a-C. During coating, the bellows were extended by approximately 20% beyond their nominal convolution length (by ≈ 15 mm) to improve the coating uniformity.

The reported values represent the average of five measurements at each location. As shown in Tables 1 and 2,

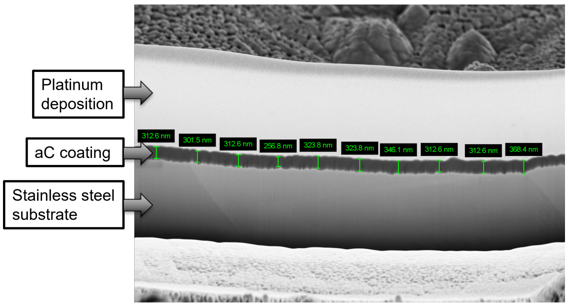

Figure 4: a-C coating thickness measured using a FIB-SEM microscope. [10]

the coating thickness is not uniform: it is greatest at the inner radius, closest to the target, and decreases by a factor of approximately 1.5–2 towards the outer radius of the convolution, which is in line with expectations. A minimum thickness of roughly 200 nm is typically required for NEG coatings, as performance in terms of number of allowable bakeout cycles degrades significantly below this threshold [11]. For a-C coatings, a minimum thickness of approximately 50 nm is typically adopted [12]. In all cases, the measured thicknesses were satisfactory.

Table 1: NEG Coating Thickness Distribution

Position	Mean (nm)	Std Dev (nm)
IR	607	74
Centre	455	52
OR	296	43

Table 2: a-C Coating Thickness Distribution

Position	Mean (nm)	Std Dev (nm)
IR	320	38
Centre	297	30
OR	214	27

An issue encountered during production, but not observed during prototyping, was NEG peel-off on the collars of two out of fourteen bellows, visible in Fig. 5. One possible cause for this is the surface finish of the collars produced by turning. Similar behaviour has previously been reported for aluminium bellow collars also manufactured by turning [13].

An action plan was established to address the affected components. The NEG coating in the damaged areas were carefully removed using a clean file, after which the bellows undergo a series of thermal and venting cycles. This should be performed at a slightly increased temperature of approximately 250 °C, above the 180 °C operational temperature used to activate the NEG for these more fragile components. This procedure is intended to determine whether the peel-off propagates or remains localised. If no further degradation is observed, the affected bellows may be considered for use in spare modules. To prevent recurrence in future production, all individual components, with the exception of the convolutions, will undergo chemical etching prior to welding. This treatment removes the oxide layer created during the welding process and increases surface roughness, improving coating adhesion.

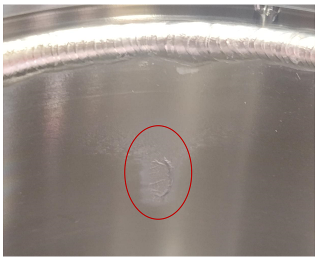

Figure 5: NEG peel-off on the collar of bellows.

ADAPTATIONS FOR REMOTE HANDLING CAPABILITIES

To ensure the M2 bellows could be manoeuvred with a robot suspended from a crane (CRANEbot), a custom flange-guiding system was developed, together with a mechanism to extend and compress the bellows during installation and maintenance, while still allowing the necessary flexibility for proper function, this is shown in Fig. 6 bellow. This solution has been extensively validated through both test bench trials and full-scale mock-up testing using the CRANEbot.

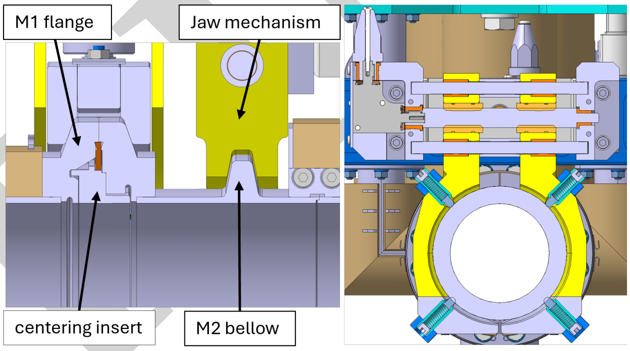

Figure 6: M2 bellows extension and centering system.

CONCLUSION

The design and production of the VAX DN80 universal joint bellows for the HL-LHC has been successfully completed, addressing the challenging mechanical and operational constraints of this region. Thin-film coatings were applied to mitigate electron cloud effects, with adhesion ensured through appropriate surface preparation. Their performance was validated through mechanical, thermal, and venting cycles beyond nominal operating conditions. Overall, the results demonstrate the feasibility of applying thin-film coatings to stainless-steel bellows and confirms that the final production meets the requirements for reliable integration and operation within the HL-LHC.

REFERENCES

[1] C. Benvenuti *et al.*, “Vacuum properties of TiZrV non-evaporable getter films”, *Vac.*, vol. 60, no. 1–2, pp. 57–65, 2001. doi:10.1016/S0042-207X(00)00246-3

[2] V. Baglin, P. Chiggiato and C. Garion, "Vacuum System", in *The High Luminosity Large Hadron Collider*, World Scientific Publishing, Ch. 17, doi:10.1142/9789811278952_0017

[3] W. Niewiem, D. Mergelkuhl, and J.-C. Gayde, "Geodetic deformation measurement and analysis of the ATLAS experimental cavern at CERN", *J. Instrum.*, vol. 17, p.11041, Nov. 2022, doi:10.1088/1748-0221/17/11/P11041

[4] R. Veness *et al.*, "Specification of New Vacuum Chambers for the LHC Experimental Interactions", in *Proc. IPAC'11*, San Sebastian, Spain, Sep. 2011, pp. 1584–1586. https://jacow.org/IPAC2011/papers/TUPS026.pdf

[5] P. Fessia and H. Mainaud Durand, "Integration, (De-) Installation and Alignment", in *The High Luminosity Large Hadron Collider*, World Scientific Publishing, Ch. 22, pp. 475–499, 2024 doi:10.1142/9789811278952_0022

[6] V. Baglin *et al.*,"HL-LHC Technical Design Report: 12. The Vacuum System for the High Luminosity LHC", *CERN Yellow Reports: Monographs*, Ch. 12.5.1, 2020. doi:10.23731/CYRM-2020-0010.229

[7] B. Salvant, "Impedance of VAX bellows options", INDICO 1016742, unpublished.

[8] E. Barnes, R. Perez Martinez, and J. Perez Espinos, "Design and calculation of the expansion joints for the HL-LHC VAX and Q1 – TAXS modules", EDMS 2915436, unpublished.

[9] V. Baglin *et al.*, "Observations of Electron Cloud Effects with the LHC Vacuum System", in *Proc. IPAC'11*, San Sebastian, Spain, Sep. 2011, pp. 1560–1562. https://jacow.org/IPAC2011/papers/TUPS018.pdf

[10] Y. Askar, "Assessing the amorphous carbon (a-C) and non-evaporable getter (NEG) coating on two bellows used in ultra-high vacuum (UHV) applications", EDMS: 3360726, unpblished.

[11] E. Belli *et al.*, " Electron cloud buildup and impedance effects on beam dynamics in the FCC-ee collider and experimental characterization of thin TiZrV vacuum chamber coatings", *Phys. Rev. Accel. Beams*, vol. 21, pp. 111002, 2018, doi:10.1103/PhysRevAccelBeams.21.111002

[12] C. Yin Vallgren *et al.*, "Low Secondary Electron Yield Carbon Coatings for Electron-cloud Mitigation in Modern Particle Accelerators", in *Proc. IPAC'10*, Kyoto, Japan, May 2010, pp. 2375–2377. https://proceedings.jacow.org/IPAC10/papers/weoamh03.pdf

[13] M. A. Gallilee *et al.*, "Development of Aluminium Vacuum Chambers for the LHC Experiments at CERN", in *Proc. IPAC'14*, Dresden, Germany, Jun. 2014, pp. 2354–2356. doi:10.18429/JACoW-IPAC2014-WEPME040